

Theory of the galvanomagnetic properties of cadmium in the temperature range 10–40°K

W. Y. Hsu* and L. M. Falicov

Department of Physics, † University of California, Berkeley, California 94720

(Received 4 June 1975)

A simple model that involves the contribution to the relaxation time of an Einstein-like phonon mode is proposed to explain recently observed puzzling features in the galvanomagnetic properties of cadmium in the temperature range from 10 to 40°K. Anisotropic scattering effects are also discussed.

I. INTRODUCTION

The galvanomagnetic properties of cadmium at low temperatures¹ are peculiar and complicated. Basically, the complication arises from the fact that different scattering mechanisms dominate the galvanomagnetic properties at different temperatures. The behavior below 4°K is well understood.² In that region, part of the hole trajectories are changed into electron trajectories because of the impurity-enhanced intersheet scattering. As a result, there is a change in the sign of the Hall coefficient. At higher temperatures, other scattering mechanisms take over and various local maxima and minima in the Hall coefficient are observed.

In this paper, we are primarily concerned with the puzzling behavior in the temperature range 10–40°K. The experiments¹ (and their analysis³) here referred to can be summarized as follows:

(i) the zero-field transverse resistivity ρ_{11} ($H=0$, T) is found to be proportional to $T^5 \mathcal{J}_5(\Theta_R/T)$, where \mathcal{J}_5 is the well-known Bloch \mathcal{J}_5 function.⁴ However, it is observed that Θ_R is approximately 109°K instead of the Debye temperature Θ_D (≈ 210 °K) as predicted by the simple Bloch theory of resistivity.⁴

(ii) For a fixed magnetic field H , $\rho_{21}(H, T)$ reaches a maximum value ρ_{21}^{\max} at a temperature T_m which lies between 10 and 20°K.

(iii) The deduced Hall coefficient $R(T)$ has the following behavior in the temperature range from 4 up to 40°K:

$$R(T)/r(T) = b \exp(-42.9/T), \quad (1.1)$$

where b is a constant independent of temperature and $r(T)$ is defined by

$$r(T) = \rho_{11}(H=0, 273\text{°K})/\rho_{11}(H=0, T). \quad (1.2)$$

(iv) If we define $\Delta\rho_{21}$ as the nonlinear contribution to the Hall resistivity

$$\rho_{21} = R(T)H + \Delta\rho_{21}, \quad (1.3)$$

it is found that $\Delta\rho_{21} \approx 0$ at $T=11$ °K, and $R(T)$ is roughly a maximum at the same temperature 11°K.

(v) Between 10 and 20°K, it is found that

$$[H/r(T)]_{\rho_{21}=\rho_{21}^{\max}} = c \exp(109/T), \quad (1.4)$$

where c is a constant independent of T .

It is also worth mentioning that in this temperature range, cadmium is restored to the state of a compensated metal in contrast to its behavior below 4°K.

In Sec. II, we present our theory, discuss the relevant features of the Fermi surface and phonon spectrum of Cd, and calculate relaxation times. The numerical results, based on four adjustable parameters (two impurity-scattering matrix elements and two electron-phonon matrix elements) are presented in Sec. III. Section IV contains our discussion and conclusions.

II. THEORY

A. General theory

We calculate the magnetoresistivity ρ_{ij} tensor under the following assumptions:

(i) The Fermi surface of Cd is topologically rather involved. Its shape and dimensions are however very well known.^{5,6} For magnetic fields parallel to the hexagonal axis, the surface behaves as if it were composed only of closed singly connected sheets. It is important to remark, however, that Cd is a compensated metal, i.e., one in which the number of electron orbits equals the number of hole orbits.⁷ In addition, from experimental measurements⁵ and calculations,⁶ it is known that the linear dimensions of the electron orbits are typically twice as large as the linear dimensions of the hole orbits. These features (and not the sixfold symmetry of the problem) are the ones which determine the galvanomagnetic properties. We therefore take a model Fermi surface to be composed of one free-electron-like pocket and compensated by eight holelike pockets, that is,

$$k_{Fe} = 2k_{Fh} \quad (2.1)$$

and

$$n_e = n_h = n, \quad (2.2)$$

where k_{Fe} , k_{Fh} are the Fermi radii for the electron and hole pockets, respectively, and n is the total

number of either type of carriers. The 8-to-1 relationship is a simple consequence of (2.1) and (2.2).

(ii) The calculation is handled in a semiclassical (Boltzmann equation) way and all quantum-mechanical coherence effects are neglected.⁸

(iii) Spatial uniformity of all physical quantities, such as temperature, electric field, and magnetic field is assumed.

(iv) The scattering term is treated in the uniform relaxation-time approximation.

(v) Only terms linear in the electric field \vec{E} (Ohm's law) are retained.

Straightforward calculations⁹ yield the following expression for the various components of the resistivity tensor:

$$\rho_{11} = \rho_{22} = \frac{1}{ne^2 \Delta} \left(\frac{\tau_e}{m_e(1 + \omega_e^2 \tau_e^2)} + \frac{\tau_h}{m_h(1 + \omega_h^2 \tau_h^2)} \right), \quad (2.3)$$

$$\rho_{21} = -\rho_{12} = \frac{1}{ne^2 \Delta} \left(\frac{\omega_h \tau_h^2}{m_h(1 + \omega_h^2 \tau_h^2)} - \frac{\omega_e \tau_e^2}{m_e(1 + \omega_e^2 \tau_e^2)} \right), \quad (2.4)$$

$$\rho_{33} = \rho_0 = \frac{1}{ne^2} \frac{1}{(\tau_e/m_e + \tau_h/m_h)}, \quad (2.5)$$

$$\rho_{13} = \rho_{23} = \rho_{31} = \rho_{32} = 0, \quad (2.6)$$

where

$$\Delta = \left(\frac{\tau_e}{m_e(1 + \omega_e^2 \tau_e^2)} + \frac{\tau_h}{m_h(1 + \omega_h^2 \tau_h^2)} \right)^2 + \left(\frac{\omega_h \tau_h^2}{m_h(1 + \omega_h^2 \tau_h^2)} - \frac{\omega_e \tau_e^2}{m_e(1 + \omega_e^2 \tau_e^2)} \right)^2, \quad (2.7)$$

ρ_0 is the zero-field resistivity, and m_e , m_h are the effective masses for the electron and hole pockets, respectively. In addition, τ_e , τ_h are separately the relaxation times for the two types of carriers, and ω_e , ω_h are cyclotron frequencies defined as

$$\omega_e = |e|H/m_e c, \quad (2.8)$$

$$\omega_h = |e|H/m_h c. \quad (2.9)$$

The above results are formally the same as that of a simple two-band model.⁹ This is because all eight hole pockets contribute additively as if it were only a single hole pocket. However, this apparent similarity is quite misleading because the effective Fermi radius for the present case of eight hole pockets is only one-half of that for a simple two-band model. As a consequence, the effective τ_h 's are different (cf., Sec. IIB) and hence the various components ρ_{ij} behave differently.

The experiments here discussed have been performed in the high-field limit, i. e., $\omega_e \tau_e \gg 1$ and $\omega_h \tau_h \gg 1$. Under such conditions, the resistivity tensor reduces to the following:

$$\rho_{11} = \rho_{22} = \frac{1}{ne^2} \left(\frac{eH}{c} \right)^2 \left/ \left(\frac{m_e}{\tau_e} + \frac{m_h}{\tau_h} \right) \right., \quad (2.10)$$

$$\rho_{21} = -\rho_{12} = \frac{H}{nec} \left(\frac{m_e}{\tau_e} - \frac{m_h}{\tau_h} \right) \left/ \left(\frac{m_e}{\tau_e} + \frac{m_h}{\tau_h} \right) \right., \quad (2.11)$$

$$\rho_{33} = \rho_0 = \frac{1}{ne^2} \left(\frac{m_e}{\tau_e} + \frac{m_h}{\tau_h} \right) \left/ \left(\frac{m_e}{\tau_e} + \frac{m_h}{\tau_h} \right) \right., \quad (2.12)$$

$$\rho_{13} = \rho_{23} = \rho_{31} = \rho_{32} = 0. \quad (2.13)$$

B. Calculation of relaxation times

The relaxation times τ_e and τ_h are calculated from the collision term $(\partial f / \partial t)_{\text{coll}}$ of the Boltzmann equation following the well-known approach of Wilson.^{4,10} In addition to the usual contribution to the relaxation time from scattering by impurities and longitudinal acoustic phonons, we introduce an additional term due to scattering by a very flat, almost Einstein-like, phonon mode. This mode is a peculiar feature of the phonon spectra of Zn and Cd.¹¹ It is a hybrid of the TA and TO modes, of practically constant frequency (2×10^{12} cps in Zn and 1.3×10^{12} cps in Cd). Such a mode is capable of scattering quasielastically electrons from any points in the Brillouin zone to any other point. In particular, it can scatter electrons from *anywhere* in the Fermi surface to any other Fermi-surface point. This flat mode is also the major cause of the relatively short Debye-like region and the huge peak just beyond the acoustic region in the phonon density-of-state distribution curve.¹¹ The typical energy of this low-lying Einstein-like mode is about one-third of the typical energy of the optical branches. As a result, we expect such mode to be equally effective in the resistive scattering of electrons. We present a separate discussion of the various contributions to the electrical resistivity in the following:

a. Impurities. As is well known, this term depends only on the number of impurities and does not depend on applied field \vec{E} and temperature,^{12,13} so

$$\tau_{\text{imp}}^{-1} = \text{const.} \quad (2.14)$$

b. Longitudinal acoustic phonons. This gives rise to the well-known Bloch T^5 term.^{4,13} However, as the calipers of the electron and hole pockets are much smaller than the size of the Brillouin zone (within the Debye approximation, the size of the zone is given by the Debye cutoff q_D), those phonons with wave vector \vec{q} such that

$$q_h < q_e < |\vec{q}| < q_D \quad (2.15)$$

are very ineffective in scattering electrons. In (2.15), q_e , q_h are, respectively, the calipers of the electron and hole pockets and are defined by

$$q_e = 2k_{Fe}, \quad (2.16)$$

$$q_h = 2k_{Fh}. \quad (2.17)$$

Physically this is because there are no available

states for the electrons to scatter into. Thus, the upper cutoff is now determined by either q_h or q_e , instead of q_D . On the other hand, the velocity of sound which comes in through the dispersion relation is still related to the Debye cutoff q_D and hence the Debye temperature Θ_D by the conservation of the total number of phonons. Thus, assuming constant electron-phonon matrix element C_D , we obtain

$$\tau_{D\text{byre}}^{-1} \propto (T/\Theta_D) \mathcal{J}_5(\Theta_{\text{cutoff}}/T), \quad (2.18)$$

where $\Theta_{\text{cutoff}} = \Theta_e$ or Θ_h with

$$\Theta_e = \hbar q_e v / k_B, \quad (2.19)$$

$$\Theta_h = \hbar q_h v / k_B, \quad (2.20)$$

and v is the velocity of sound, while \hbar and k_B are Planck's and Boltzmann's constants, respectively. In the actual numerical fitting, Θ_e and Θ_h are estimated from the Zn dispersion curve by scaling, since neutron scattering data for Cd are not available.

c. Einstein-like phonon. The energy of this mode, like the energy of any phonon mode, can be neglected as compared with typical electronic energies (in the order of Fermi energy). Yet, it can supply a very large momentum transfer. Thus, it is not only effective in causing further intraelectron and intrahole scattering, but also capable of scattering electrons into hole pockets and *vice versa*, as well as causing transitions between different hole pockets. The matrix elements for these processes $C_{\text{intra-e}}$, $C_{\text{intra-h}}$, C_{e-h} , and $C_{\text{inter-h}}$ are, in general, different. For simplicity, we assume all four of them to be equal and constant, that is,

$$C_{\text{intra-e}} = C_{\text{intra-h}} = C_{e-h} = C_{\text{inter-h}} = C_E. \quad (2.21)$$

Then, for each case, we obtain

$$\tau_{E\text{inst.}}^{-1} \propto [\exp(\Theta_E/T) - 1]^{-1}, \quad (2.22)$$

where

$$\Theta_E = \hbar \omega_E / k_B \quad (2.23)$$

and $\hbar \omega_E$ is the energy of the Einstein-like phonon. The above result has an immediate physical interpretation as it simply reflects the fact that the scattering probability is determined by the phonon distribution. The more phonons there are, the more electrons they can scatter. On the other hand, the hole-hole and electron-hole transitions as caused by acoustic phonons are energetically unfavorable, because the energy involved is of the order of $k_B \Theta_D$.

The inclusion of all these terms yields

$$\tau_e^{-1} = C_e + A [m_e / (k_{Fe} a)^3] (T/\Theta_D) \mathcal{J}_5(\Theta_e/T) + B(m_e k_{Fe} a + 8m_h k_{Fh} a) [\exp(\Theta_E/T) - 1]^{-1}, \quad (2.24)$$

$$\tau_h^{-1} = C_h + A [m_h / (k_{Fh} a)^3] (T/\Theta_D)^5 \mathcal{J}_5(\Theta_h/T)$$

$$+ B(m_e k_{Fe} a + 8m_h k_{Fh} a) [\exp(\Theta_E/T) - 1]^{-1}, \quad (2.25)$$

where C_e , C_h are constant impurity terms and a is the lattice constant. In addition,

$$A = 9\pi^3 (C_D^2 / \hbar) (1/k_B \Theta_D) (1/M) \alpha, \quad (2.26)$$

$$B = (1/\pi) (C_E^2 / \hbar) (1/k_B \Theta_E) (1/M) \beta, \quad (2.27)$$

with M the ionic mass, α , β are the fractions of the phonon spectrum corresponding to the Debye and Einstein modes, respectively, and C_D and C_E are constant matrix elements involved in the scattering of electrons by the two modes, respectively. The constants A , B , C_e , and C_h are taken as adjustable parameters.

Equations (2.10)–(2.13) together with (2.24) and (2.25) enable us to describe completely the magnetoresistivity tensor ρ_{ij} .

III. NUMERICAL CALCULATION

We calculate the Hall coefficient $R(T)$, zero-field resistivity, and the ratio $R(T)/r(T)$ for various contributions of A , B , C_e , and C_h . For convenience, the actual parameters that we have adjusted in our numerical investigation are multiples of A , B , C_e , and C_h as defined by

$$A' = m_e^2 [1/(k_{Fe} a)^3] (\Theta_e / \Theta_D)^5 A, \quad (3.1)$$

$$B' = m_e^2 (k_{Fe} a) B, \quad (3.2)$$

$$C'_e = m_e C_e, \quad (3.3)$$

and

$$C'_h = m_h C_h. \quad (3.4)$$

The numerical values of other relevant physical quantities as used in the present calculation are summarized as follows: (i) electron and hole calipers⁵

$$k_{Fe} = 2k_{Fh} \cong 0.7 \text{ \AA}^{-1};$$

(ii) effective masses¹⁴

$$m_e = 1.3m_0$$

and

$$m_h = 0.2m_0,$$

where m_0 is the mass of a free electron; (iii) cadmium ionic mass¹⁵

$$M = 112.4 \text{ amu};$$

(iv) average size of unit cell^{15,16}

$$a = 6.36 \text{ \AA};$$

(v) Debye temperature¹⁷

$$\Theta_D = 210 \text{ }^\circ\text{K};$$

(vi) characteristic temperature for the Einstein-like mode, Θ_E : taken to be either 54 °K or 60 °K¹⁸; and (vii) characteristic cutoff temperature for the

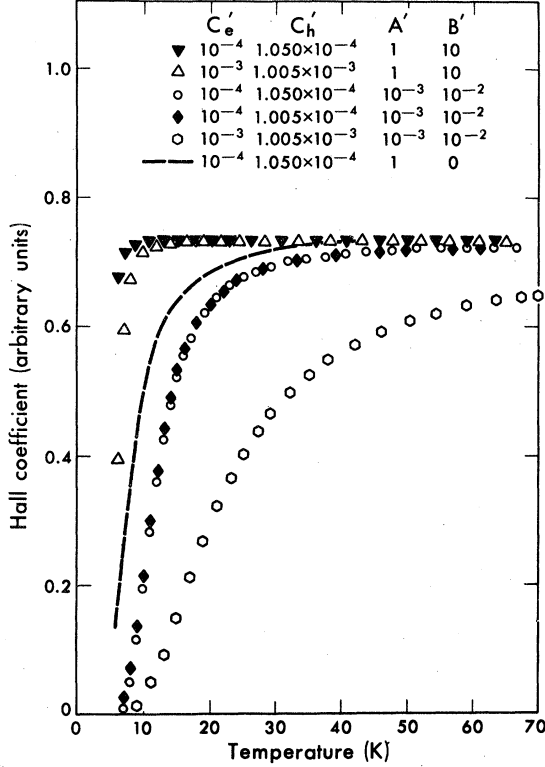


FIG. 1. Temperature variation of the Hall coefficient for the isotropic scattering model. Different values of the parameters C'_e , C'_h , A' , and B' are shown on the graph. In this case, Θ_E is taken to be 54°K.

electron and hole pockets¹⁸

$$\Theta_h = 77.6 \text{ }^\circ\text{K},$$

$$\Theta_e = 105 \text{ }^\circ\text{K}.$$

Typical results are shown graphically in Figs. 1-3. We can explain basically the rise in $R(T)$ around 10°K, the behavior of $\rho_0(T)$ and $R(T)/r(T)$. However, within the assumptions of isotropic and constant matrix elements (2.21), we are unable to account for the drop in $R(T)$ beyond 11°K. It is straightforward to generalize our equations to handle anisotropic cases. For the sake of clarity, we present here our results of one special limit: the case in which $C_{\text{inter-h}}$ is constant and much larger than the other three matrix elements. This corresponds to a situation where the Einstein-like phonon mode is only effective in interhole scattering but quite inefficient in intrahole, intraelectron, and electron-hole scattering. Equations (2.24) and (2.25) now take the following forms:

$$\tau_e^{-1} = C_e + A[m_e / (k_{F_e} a)^3] (T/\Theta_D)^5 \mathcal{J}_5(\Theta_e/T), \quad (3.5)$$

$$\tau_h^{-1} = C_h + A[m_h / (k_{F_h} a)^3] (T/\Theta_D)^5 \mathcal{J}_5(\Theta_h/T) + 7Dm_h k_{F_h} a [\exp(\Theta_E/T) - 1]^{-1}, \quad (3.6)$$

where D is defined in a similar way to B .

$$D = (1/\pi)(C_{\text{inter-h}}^2/\hbar)(1/k_B \theta_E)(1/M)\beta. \quad (3.7)$$

We also define

$$D' = 7m_h k_{F_h} a D. \quad (3.8)$$

Our calculation shows that the behavior of $\rho_0(T)$ and $R(T)/r(T)$ are similar to those of the isotropic case [Figs. 4(b) and 4(c)]. On the other hand, the agreement of $R(T)$ with the experimental results improves drastically. The calculated Hall coefficient now exhibits a local maximum in the temperature range 10–30°K depending on the value of our parameters. Typical results are shown in Fig. 4(a).

IV. CONCLUSIONS AND DISCUSSION

Our results can be summarized as follows:

(i) Experimental results can be understood qualitatively as well as quantitatively by the inclusion of anisotropic scattering of electrons by a very flat, almost Einstein-like phonon mode, a hybrid of TA and TO branches.

(ii) Within the isotropic scattering model, the combined effect of Debye and Einstein phonons is to cause a sharp rise in the Hall coefficient in the

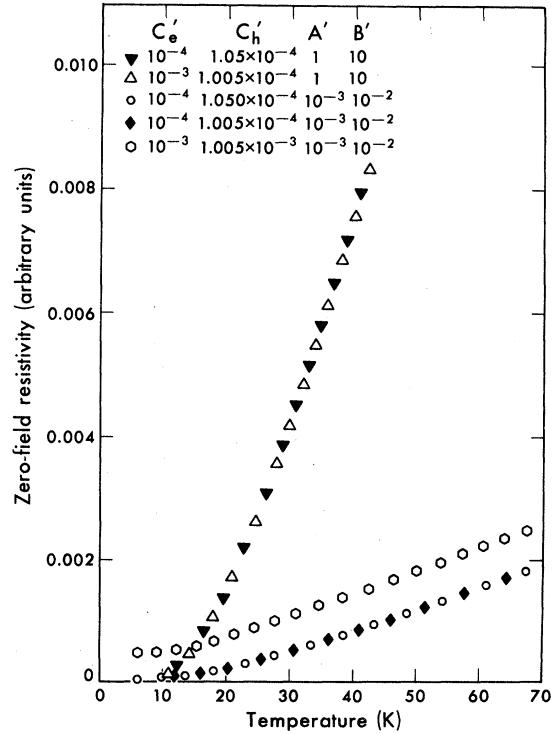


FIG. 2. Temperature variation of the zero-field resistivity for the isotropic scattering model with the characteristic temperature of the Einstein-like mode Θ_E taken to be 54°K.

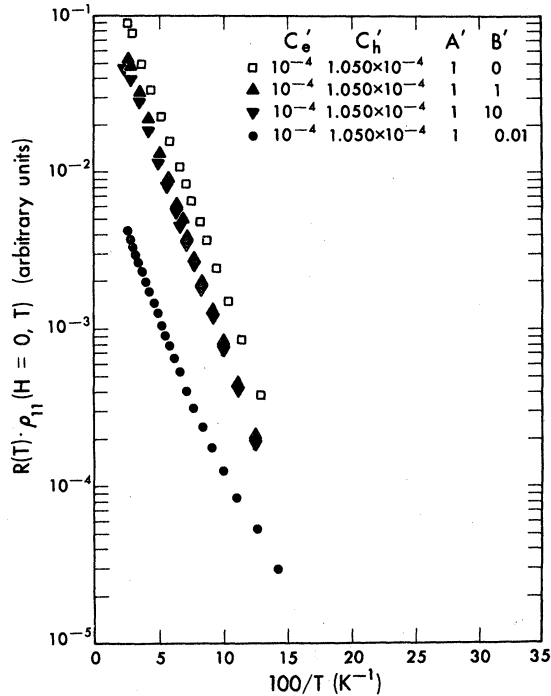


FIG. 3. Semilogarithmic plot of the product of the Hall coefficient and the zero-field resistivity as a function of $100/T$ for the isotropic scattering model with a Θ_E equal to 54°K .

neighborhood of $10\text{--}20^\circ\text{K}$ with a line shape which compares favorably to the experimental one. Bloch T^5 terms alone caused too slow a rise and the Einstein term alone drops too steeply. If the impurity term is too large so as to be dominant, the rise is again very slow; in such a case, the

impurity contributions dominate both in numerator and denominator and tend to maintain the constant value

$$(C'_e - C'_h)[\text{neq}(C'_e + C'_h)]^{-1}.$$

Our fully isotropic model, however, cannot explain the drop in the Hall coefficient beyond 20°K . Our calculation evidently yields a constant plateau in that range, in disagreement with the experimental results.

(iii) This phenomenon of a local maximum in the Hall coefficient can be adequately accounted for if anisotropic scattering is properly incorporated. In fact, the experiments here discussed provide a direct measure of such anisotropy.

(iv) $R(T)/r(T)$ as plotted against $100/T$ in a semilog scale also appears to be linear in the temperature range $4\text{--}40^\circ\text{K}$ for both the isotropic and anisotropic scattering models. A plot of $1/r(T)$ alone deviates considerably from the straight line but not as drastically as observed experimentally.

For the values of A' , B' , C'_e , and C'_h that we have used, the same linear behavior is observed and the slope varies from 42 to 48°K , which compares favorably to the observed 43°K .

(v) The observed deviation of the zero-field resistivity from that of a simple Bloch model is due to (a) the existence of both electron and hole pockets of different sizes which have very different scattering parameters, (b) the existence of a term due to the Einstein-like phonon mode, and (c) the very small value of the mass ratio m_h/m_e . All these factors combine to cause an apparent fit to a single Bloch \mathcal{J}_e function with scaling parameters approximately equal to $\frac{1}{2}\Theta_D$ as observed experi-

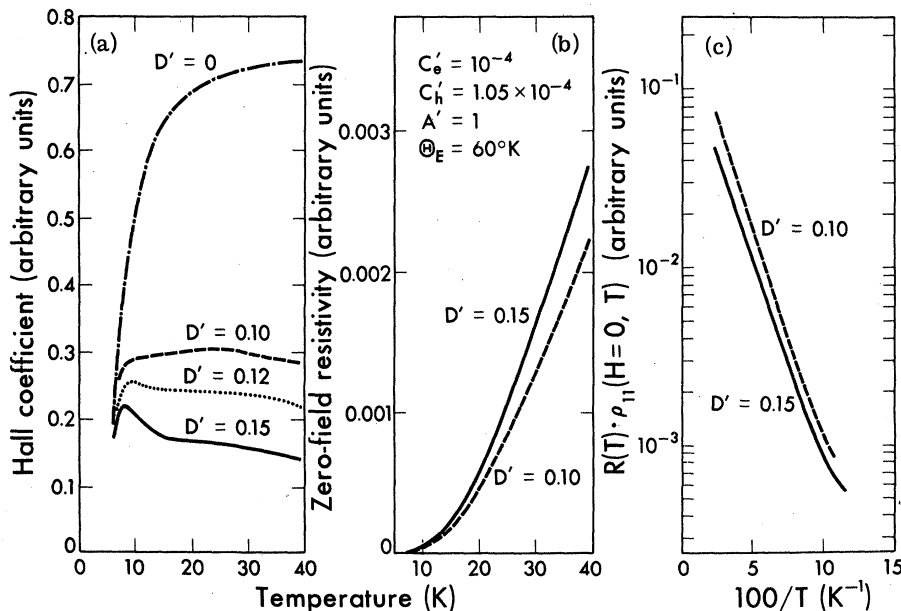


FIG. 4. Galvanomagnetic properties of the anisotropic scattering model for different values of the parameter D' and fixed value of the parameters C'_e , C'_h , A' , and Θ_E . (a) Hall coefficient as a function of temperature. Case $D' = 0$ corresponds to the case $B' = 0$ in Fig. 1. (b) Zero-field resistivity as a function of temperature. (c) Semilogarithmic plot of the product of the Hall coefficient and the zero-field resistivity as a function of $100/T$.

mentally.

(vi) Because of the other approximations employed in this calculation, we feel that a more realistic treatment of the Fermi surface is somewhat meaningless. A much more sensible approach would be the use of a variational technique.¹⁹

(vii) In spite of the shortcomings of the present approach, our calculation does confirm the im-

portance of the Einstein-like phonon mode which has always been overlooked.

ACKNOWLEDGMENT

The authors would like to thank Professor Gerritsen for calling our attention to this problem and for several very illuminating discussions.

*I. B. M. Predoctoral Fellow.

†Work supported in part by the NSF through Grant No. DMR72-03106-A01.

¹D. A. Lilly and A. N. Gerritsen, Phys. Rev. B **9**, 2497 (1974); Physica (Utr.) **69**, 286 (1973), and references therein.

²R. A. Young, J. Ruvalds, and L. M. Falicov, Phys. Rev. **178**, 1043 (1969).

³A. N. Gerritsen, Phys. Rev. B **12**, xxxx (1975).

⁴A. H. Wilson, *The Theory of Metals*, 2nd ed. (Cambridge University, New York, 1965), Chap. 9.

⁵R. C. Jones, R. G. Goodrich, and L. M. Falicov, Phys. Rev. **174**, 672 (1968).

⁶R. W. Stark and L. M. Falicov, Phys. Rev. Lett. **19**, 795 (1967).

⁷E. Fawcett, Adv. Phys. **13**, 139 (1964).

⁸L. M. Falicov, in *Electrons in Crystalline Solids* (International Atomic Energy Agency, Vienna, 1973), p. 250.

⁹J. M. Ziman, *Principles of the Theory of Solids*, 2nd ed. (Cambridge University, Cambridge, 1972), p. 250ff.

¹⁰R. E. Peierls, *Quantum Theory of Solids* (Oxford University, Oxford, 1965), Chap. 6.

¹¹L. J. Raubenheimer and G. Gilat, Phys. Rev. **157**, 586 (1967).

¹²J. M. Ziman, *Principles of the Theory of Solids*, 2nd ed. (Cambridge University, Cambridge, England, 1972), p. 220.

¹³J. M. Ziman, *Electrons and Phonons* (Oxford University, Oxford, 1963), Chap. 9.

¹⁴M. P. Shaw, T. G. Eck, and D. A. Zych, Phys. Rev. **142**, 406 (1966).

¹⁵C. J. Smithells, *Metal Reference Book* (Butterworths, London, 1967).

¹⁶The volume of unit cell is $V = 3\sqrt{3}(2.973)^2(5.605) \text{ \AA}^3$, and our averaged value of a is given by $a = V^{1/3}$.

¹⁷T. C. Cetas, J. C. Holste, and C. A. Swenson, Phys. Rev. **182**, 679 (1969).

¹⁸Values for the cadmium case are obtained from those of Zn as given in Ref. 8 by scaling. The resulting values are roughly the same regardless of whether we scale them by their velocity of sounds or their Debye temperatures. The scaling factor is between 0.6 and 0.7.

¹⁹R. E. Peierls, *Quantum Theory of Solids* (Oxford University, Oxford, 1965), Chaps. 7 and 12.